

THE COSMIC MICROWAVE BACKGROUND ANISOTROPY POWER SPECTRUM FROM THE BEAST EXPERIMENT

IAN J. O'DWYER,¹ MARCO BERSANELLI,² JEFFREY CHILDERS,^{3,4} NEWTON FIGUEIREDO,⁵ DORON HALEVI,^{3,4} GREG HUEY,^{1,6}
PHILIP M. LUBIN,^{3,4,7} DAVIDE MAINO,² NAZZARENO MANDOLESI,⁸ JOSHUA MARVIL,^{3,4} PETER R. MEINHOLD,^{3,4,7}
JORGE MEJÍA,⁹ PAOLO NATOLI,¹⁰ HUGH O'NEILL,^{3,4} AGENOR PINA,⁵ MICHAEL D. SEIFFERT,¹¹
NATHAN C. STEBOR,^{3,4,7} CAMILO TELLO,⁹ THYRSO VILLELA,⁹ BENJAMIN D. WANDEL,^{1,6}
BRIAN WILLIAMS,^{3,7} AND CARLOS ALEXANDRE WUENSCHÉ⁹

Received 2003 December 23; accepted 2005 January 10

ABSTRACT

The Background Emission Anisotropy Scanning Telescope (BEAST) is a 2.2 m off-axis telescope with an eight-element mixed Q-band (38–45 GHz) and Ka-band (26–36 GHz) focal plane, designed for balloon-borne and ground-based studies of the cosmic microwave background (CMB). Here we present the CMB angular power spectrum calculated from 682 hr of data observed with the BEAST instrument. We use a binned pseudo- C_l estimator (the MASTER method). We find results that are consistent with other determinations of the CMB anisotropy for angular wavenumbers l between 100 and 600. We also perform cosmological parameter estimation. The BEAST data alone produce a good constraint on $\Omega_k \equiv 1 - \Omega_{\text{tot}} = -0.074 \pm 0.070$, consistent with a flat universe. A joint parameter estimation analysis with a number of previous CMB experiments produces results consistent with previous determinations.

Subject headings: cosmic microwave background — cosmology: observations — large-scale structure of universe

Online material: color figure

1. INTRODUCTION

Understanding the mechanisms of structure formation in the early universe ($10 < z < 1000$) is one of the most important and active areas in cosmology today, and measurements of the cosmic microwave background (CMB) anisotropy play a pivotal role in this field. In the framework of the standard cosmological model, the CMB radiation is interpreted as the blackbody radiation associated with a hot dense phase of the universe, when matter and radiation were in thermal equilibrium (e.g., Peebles 1993). On large angular scales the CMB radiation traces the primordial power spectrum set by physical processes during the first instants after the big bang. On smaller angular scales, CMB anisotropies are influenced by factors that control the expansion rate of the universe and formation of large-scale structure, such as the cosmological constant, the matter density, and the existence and nature of dark matter (e.g., Kolb & Turner 1990). By measuring the angular power spectrum of CMB fluctuations, one can

discriminate among various competing theories that predict the primordial mass distribution (e.g., inflation, cosmic strings and textures, and primordial isocurvature baryonic perturbations) and understand the gravitational collapse that ultimately brought about the formation of galaxies. Since the fluctuation amplitudes at angular scales of a few degrees and smaller are also sensitive to the free electron distribution, CMB measurements can also be used to determine the ionization history of the universe.

After the release of the *WMAP* (*Wilkinson Microwave Anisotropy Probe*) full-sky data (Bennett et al. 2003), suborbital CMB anisotropy experiments are still of high scientific interest as they can improve angular resolution and sensitivity over limited sky regions. The Background Emission Anisotropy Scanning Telescope (BEAST) is the only project currently on-going that is probing a frequency range overlapping with that of *WMAP*, with improved angular resolution (up to 0.38° at ~ 40 GHz) and over approximately 5% of the sky. The experiment is installed in a conventionally accessible, high-altitude site and it has so far accomplished three observing campaigns, on which this paper is based. In this paper we discuss the constraints BEAST places on the power spectrum of CMB anisotropies and its consistency with data taken from a subset of previous experiments (MAXIMA, Hanany et al. 2000; TOCO, Miller et al. 1999; BOOMERANG, Ruhl et al. 2002; DASI, Halverson et al. 2001; VSA, Grainge et al. 2003; ACBAR, Kuo et al. 2002; CBI, Padin et al. 2001; *WMAP*, Bennett et al. 2003).

We present a brief overview of the experiment in § 2 and an overview of the estimator in § 3. Section 4 details our implementation of the estimator for the BEAST data, and § 5 presents the power spectrum and the parameter estimation. We summarize the results in § 6.

2. THE BEAST EXPERIMENT

BEAST is a 2.2 m off-axis telescope, currently configured with an eight-element mixed Q-band (38–45 GHz) and Ka-band

¹ Astronomy Department, University of Illinois at Urbana-Champaign, Urbana, IL 61801-3074.

² Physics Department, University of Milano, via Celoria 16, 20133 Milano, Italy.

³ Physics Department, University of California, Santa Barbara, CA 93106.

⁴ UC Santa Barbara Center for High Altitude Astrophysics at White Mountain.

⁵ Universidade Federal de Itajubá, Departamento de Física e Química, Caixa Postal 50 37500-903—Itajubá, MG, Brazil.

⁶ Department of Physics, University of Illinois at Urbana-Champaign, Urbana, IL 61801-3080.

⁷ University of California, White Mountain Research Station, CA 93514.

⁸ IASF-CNR sezione di Bologna, via P.Gobetti, 101, 40129 Bologna, Italy.

⁹ Instituto Nacional de Pesquisas Espaciais, Divisão de Astrofísica, Caixa Postal 515, 12245-970—São José dos Campos, SP, Brazil.

¹⁰ Dipartimento di Fisica e sezione INFN, Università di Roma “Tor Vergata,” Rome, Italy.

¹¹ Jet Propulsion Laboratory, California Institute of Technology, Oak Grove Drive, Pasadena, CA 91109.

(26–36 GHz) focal plane, and a modulating flat mirror. BEAST was designed as a high-altitude balloon system and had two flights: 2000 May 20–21 and October 16. Subsequent to the second flight BEAST was reconfigured to take advantage of the UC White Mountain Research Station, Barcroft Station, at an altitude of 3.8 km in the Eastern Sierra of California. The instrument was fully installed and operational at Barcroft in 2001 July and took data nearly continuously until 2001 December (except for days lost to weather and several equipment failures due to power surges and lightning). Two more weeks of data were obtained in 2002 February. A second data taking campaign proceeded in August and September of 2002. The data used for determining the power spectrum presented in this paper are taken from all three of these campaigns.

The data presented in this paper were gathered using the BEAST telescope in a fixed elevation mode. The telescope is kept at a fixed elevation near 90° and the rotation of the Earth provides the map scanning. This strategy results in a sky coverage that forms an annulus centered on the north celestial pole. The annulus is 9° wide and is located between 33° and 42° in declination.

Other aspects of the BEAST experiment are described in the accompanying papers. The instrument is described in Childers et al. (2005), and a more detailed discussion of the optics can be found in Figueiredo et al. (2005). The mapmaking procedure is described in Meinhold et al. (2005), and constraints on Galactic foregrounds in Mejia et al. (2005).

3. THE MASTER METHOD

We extract the CMB power spectrum from the BEAST data using the MASTER method, a binned pseudo- C_l estimator (Wandelt et al. 2001; Hivon et al. 2002). We chose this estimator for its ease of implementation and the flexibility it offers, which allows testing the analysis with a number of cuts and filtering schemes designed to remove Galactic, terrestrial, and instrumental foregrounds.

The MASTER method is a debiasing scheme calibrated against Monte Carlo simulations. Pseudo- C_l are calculated on the noisy maps over the observed region on the sky with no corrections made for the effect of this cut in terms of the couplings introduced between spherical harmonic modes. The expectation values of these pseudo- C_l are modeled in terms of an *Ansatz* which involves, as parameters, an instrumental transfer function F_l and a noise bias term N_l . These terms are estimated from Monte Carlo simulations of CMB signal and of experimental noise.

The signal and noise are simulated by taking separate random realizations of pure CMB signal and realistic simulations of experimental noise and subjecting them separately to exactly the same data processing (such as beam smoothing, scanning, cuts in the time-ordered data, filtering, template removal, and mapmaking) as the real data. The power spectra of the resulting signal and noise maps are averaged over the Monte Carlo runs to produce expectation values of the signal-only and noise-only power spectra. These are used to compute the transfer function and noise bias terms in the pseudo- C_l estimator. To the extent to which the MASTER *Ansatz* models the expectation values of the pseudo- C_l and to which our Monte Carlo procedure mimics the acquisition of the real data, we are guaranteed an unbiased power spectrum result.

The experimental data are now passed through the data processing pipeline and the pseudo- C_l are calculated. Since the experiment covers only a fraction of the sky, a coupling is introduced when performing the spherical harmonic transforms to calculate the power spectra. By calculating the mode-mode

coupling kernel for the observed unmasked region on the sky, it is possible to correct for this effect.

Finally, a binning scheme is chosen in l for the final power spectrum and a number of Monte Carlo simulations containing both signal and noise are performed. The covariance matrix of the estimates is calculated by computing the pseudo- C_l estimator on these simulations. The diagonal elements of the binned covariance matrix are the variances of the binned power spectrum.

4. IMPLEMENTATION OF MASTER FOR BEAST

In order to produce an accurate CMB power spectrum from the BEAST data, a detailed knowledge of the experimental beam shape and pointing is required.

Comparison of the amplitude and morphology of Cygnus A in our maps with simple Gaussian simulations of the beam leads us to conclude that it is well modeled by a circularly symmetric Gaussian profile with an effective FWHM of $23' \pm 1'$. The measured telescope resolution is $19' \pm 2'$. The smearing from the design resolution to the measured effective FWHM of $23'$ is due to a combination of unmeasured pointing errors (telescope flex, long-term telescope sag), residual errors in the pointing reconstruction algorithm, smearing due to the finite HEALPix resolution of $6.9'$, and smearing from the initial flat rotation sectors (about $6.7'$). For more detail see Meinhold et al. (2005). We use the pointing information reconstructed from a pointing model, which is included in the raw data files, to project our simulations onto the sky in the same manner that the real data are scanned.

A total of 682 individual hours of experimental data are used for the analysis. The data are naturally divided into 55 minute sections by our hourly calibration cycles. These 55 minute sections are a useful size for several reasons. In addition to the natural delineation by calibrations, 55 minutes is a very manageable size for manipulation in the IDL software package on a desktop computer. In addition, sky rotation over 1 hr at our observing angle provides redundant scanning over a nearly symmetric sky patch. The most important effect of this choice of 55 minutes is on our atmospheric offset subtraction described below. We tested the sensitivity of our results to varying the timescale of our atmospheric offset removal from the fiducial hour down to a minimum (set by sky rotation) of 600 s and observed no significant changes.

The data have been inspected, and spurious signal events, e.g., due to aircraft, have been removed. The data include both the signal measured by the experiment and the experimental pointing at that instant. This information is used to construct a sky map of the observed signal. For all the maps created in the data analysis we use the HEALPix¹² (Górski et al. 1998) pixelization scheme with an NSIDE parameter of 512. This results in a map containing 3,145,728 pixels. Given the size of the experimental beam and the high sampling frequency that is possible with a ground-based instrument (450 Hz for BEAST), the effects of pixel smoothing are negligible and are ignored here. For the experimental data we create a HEALPix map and calculate the CMB power spectrum using the HEALPix ANAFast package. Further details of the mapmaking process can be found in Meinhold et al. (2005). Figure 1 shows an overview of the steps in the BEAST simulation and analysis pipeline.

A foreground mask is applied to remove the Galaxy and point source contamination from known sources. We remove from the analysis all pixels with latitude $|b| \leq 17.5^\circ$. We tested the analysis pipeline with a range of Galactic latitude cuts and found

¹² See <http://www.eso.org/science/healpix/>.

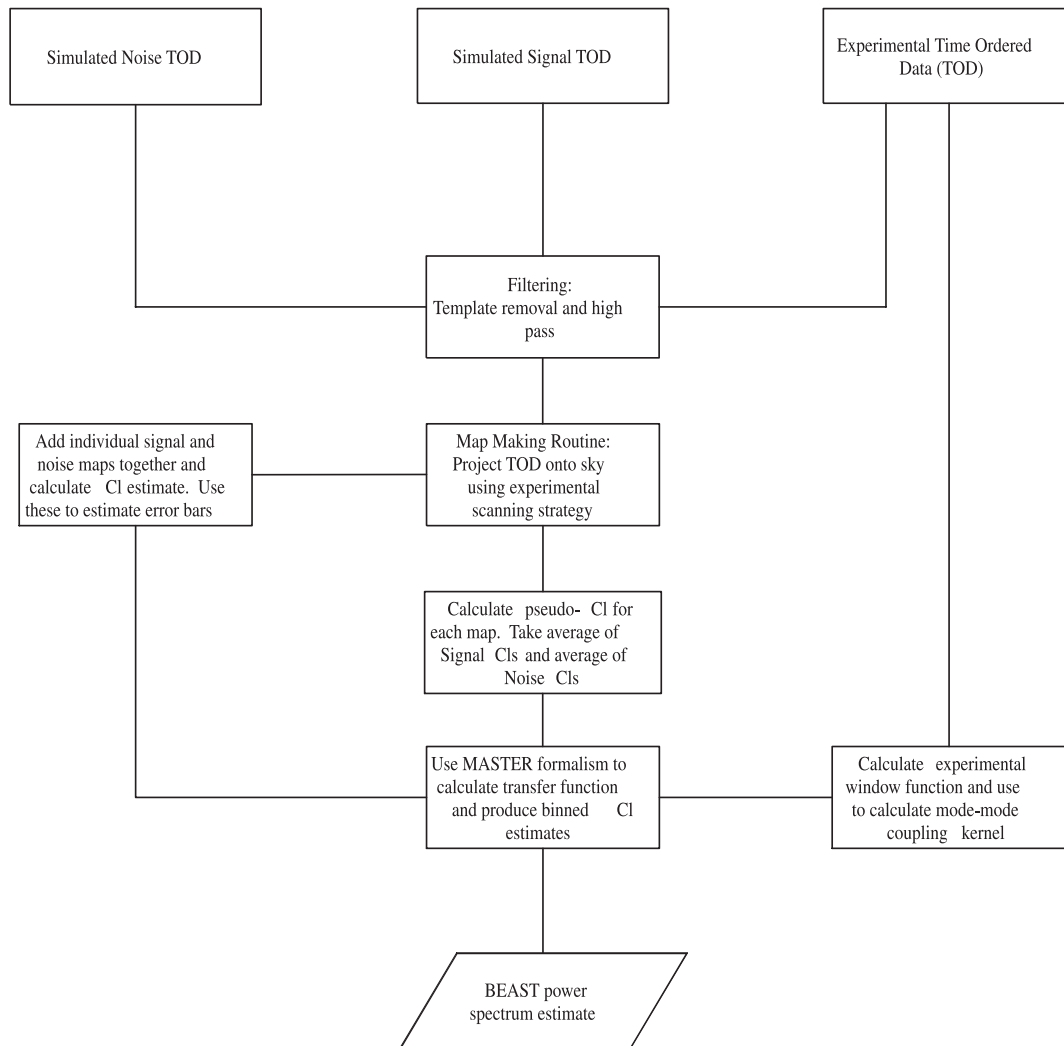


FIG. 1.—Overview of the steps in the BEAST simulation and analysis pipeline.

that below $|b| = 17.5$ there was significant Galactic foreground contamination, whilst above this Galactic latitude our results were relatively insensitive to the choice of the cut. In addition to this, a separate analysis of the Galactic foregrounds for the BEAST experiment (Mejía et al. 2005) calculated the percentage contribution of each foreground to the observed temperature of the CMB in both the Q and Ka bands. It was found that using a mask for $|b| \leq 17.5$ gives an optimal compromise between maximizing the sky fraction observed by the experiment and minimizing the amount of foreground contamination. In this work it was also found that residual Galactic foregrounds outside the mask are small, and they are ignored here.

In order to remove the contaminating effects of point sources, we have used a simple algorithm to identify potential sources in the BEAST field. First, the raw data map was smoothed with a $20'$ FWHM Gaussian. All pixels in this smoothed map with at least 100 observations and a data value (corrected for smoothing) at least 3 times the noise level were flagged. The noise level at each pixel was estimated from the ensemble of measurements at each pixel. A potential source was identified with the local maximum of neighboring marked pixels. There were 12 potential sources thus identified in the region $|b| > 17.5$. Several of these have positions coincident with bright 3C radio sources and have fluxes of several Jy; others are probably false triggers caused by noise fluctuations. Pixels within a 1° diameter circle

centered on each potential source were flagged and were excluded from the subsequent power spectrum analysis pipeline. The positions of these are evident in Figure 2.

We tested the BEAST pipeline with the power spectra from two fiducial cosmological models and found the final power spectrum to be unchanged by this choice. The first model was a set of reasonable current estimates for cosmological parameters prior to the *WMAP* data release, and the second was the best-fit power spectrum published by the *WMAP* team (Bennett et al. 2003). For the final analysis, the *WMAP* power spectrum is used to create random realizations of the pure CMB sky.

We scan these signal maps using our experimental pointing strategy read from the time-ordered data (TOD) files. We expect the time-averaged atmospheric contributions to the data to vary with elevation. To remove this foreground we fit a function of elevation angle to the TOD for each hour and subtract it from the TOD samples. Subsequently, a 10 Hz high-pass filter is used. The simulation has now been subjected to exactly the same scanning and filtering as the real BEAST data, and we project this simulated data back onto a sky map.

Finally, a power spectrum is generated from each signal map, and these power spectra are averaged to produce an average signal-only power spectrum.

To construct noise-only maps we subtract our signal estimate for the map from each sample in the experimental TOD and

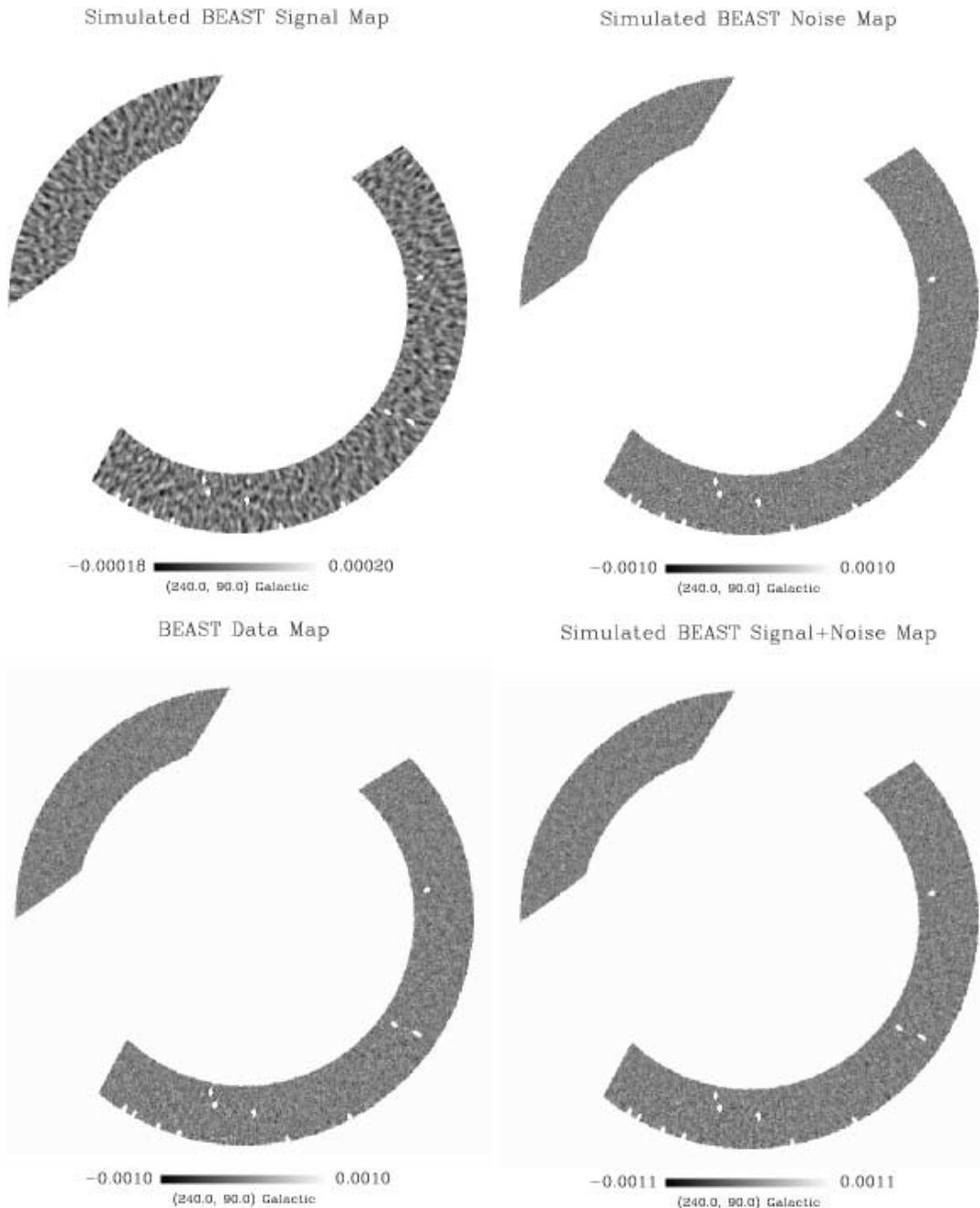


FIG. 2.—Comparison of simulated and actual BEAST maps in units of kelvin. The noise-dominated nature of the BEAST data can be seen by comparing the noise map to the BEAST data map.

assume that each hourly segment of experimental data is now noise-dominated. We further assume the noise to be piecewise stationary over one-hour sections of data and that each one-hour noise chunk is independent. We estimate noise power spectra using a windowed FFT on each hourly segment (Press et al. 1986). We are then able to generate synthetic noise simulations that have the same power spectrum as the actual noise from the experiment. We filter the simulated noise TOD in the same manner as for the data and signal simulations and project the noise onto a sky map, then calculate the average noise power spectrum. Comparisons of the data map and the maps created in the simulation pipeline are shown in Figure 2.

Since we have all of the pointing information, we can also create the experimental window function on the sky. This is a simple geometrical construction that is 1 for any HEALPix

pixel the experiment observes and 0 elsewhere. We use this window function to calculate the mode-mode coupling kernel, $M_{ll'}$, which depends only on the geometry of the observed region of sky. We use the *Ansatz* for the expected pseudo- C_l , which was proposed in Hivon et al. (2002). From the signal-only simulations we can calibrate the transfer function

$$F_l = M_{ll'}^{-1} \langle C_{ls} \rangle \langle C_l \rangle^{-1} (B_l^2)^{-1},$$

where $\langle C_{ls} \rangle$ are the signal-only pseudo C_l and $\langle C_l \rangle$ are the best-fit theory C_l from the *WMAP* experiment; B_l is the experimental beam, a Gaussian with FWHM of $23'$ in this case. Since the coupling kernel is ill-conditioned, we use an iterative approach for computing $M_{ll'}^{-1} \langle C_{ls} \rangle$. The transfer function for the BEAST experiment is shown in Figure 3.

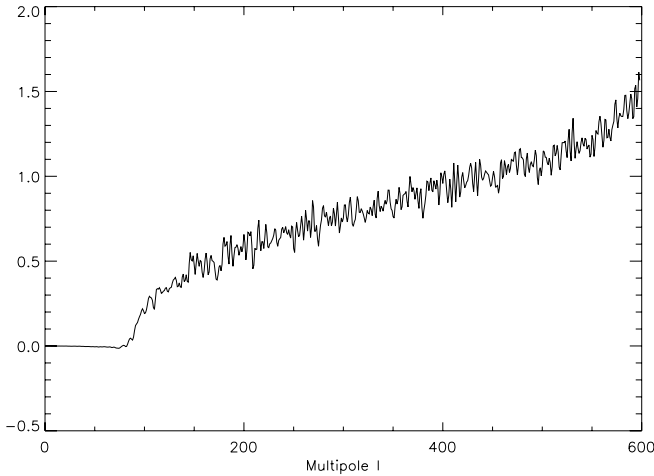


FIG. 3.—Unbinned transfer function for BEAST. Monte Carlo noise is visible, which is smoothed by the binning process. The turnover at $l \sim 550$ is caused by the ill-conditioned mode-mode coupling kernel.

Now our C_l estimate is given by

$$\hat{C}_l = \frac{M_{ll}^{-1} \tilde{C}_l - \langle \tilde{N}_l \rangle}{F_l B_l^2}$$

where $\langle \tilde{N}_l \rangle$ are the pseudo- C_l from the noise Monte Carlo simulations and \tilde{C}_l are the pseudo- C_l from the data.

In practice we use the binned version of the above equation as given in Hivon et al. (2002). The binned mode-mode coupling kernel is shown in Figure 4.

By averaging the power spectrum over bins in l we effectively reduce correlations between the C_l bins that were introduced by the sky cut and we also reduce the errors on the resulting power spectrum estimator. We have tried different binning schemes and choose a bin width of $\Delta l = 55$. The width of the diagonal band in the mode-mode coupling kernel is approximately 50 elements in l space. In order to produce uncorrelated l -bins we require a bin width of at least this size. A bin width of 55 assures us of this, whilst allowing us to get an almost maximal number of binned points in the power spectrum.

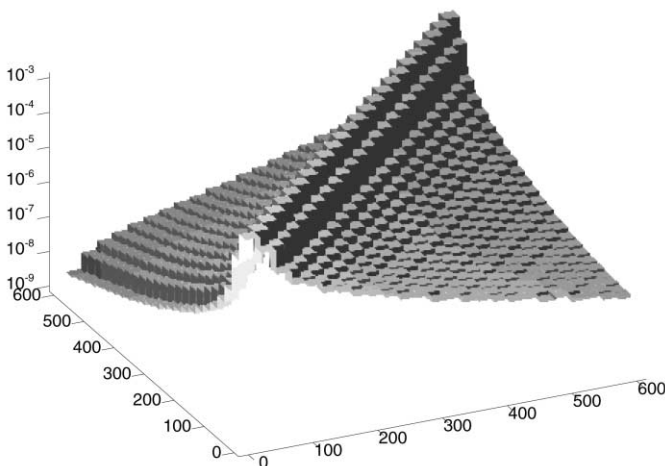


FIG. 4.—Mode-mode coupling kernel for the BEAST experiment. The z-axis is logarithmically scaled in order to show the off diagonal elements, which decrease rapidly. The width of the diagonal is approximately 25 in l either side of the peak. In order to avoid correlations between the bins in our final power spectrum, we therefore choose a bin width of 55 in l .

Finally, we create sky simulations by adding the signal and the noise maps, produced as described above. The covariance matrix $C_{bb'}$ of the binned power spectrum is calculated from these simulations and the diagonal elements give us the error bars on the binned power spectrum estimator. The power spectrum obtained from this process is discussed in the next section.

At various stages in the pipeline we have tested for systematic errors. For example, checks were performed for atmospheric and electrical noise at the TOD and map level. We have also conducted jack-knife analyses on different cuts of the data. We compared the power spectra obtained from maps of the first half of the data against the second half and odd-numbered hours against even-numbered hours. None of these tests indicated the presence of significant residual systematic error in the maps or power spectrum.

Calibration uncertainties for BEAST are dominated by uncertainties in atmospheric temperature and limited by the lack of celestial calibration sources in our region of the sky, with the exception of Cygnus A. Based on calibration tests with Cygnus A, we estimate our calibration uncertainty to be $\pm 6\%$. The calibration of the instrument is discussed fully in Childers et al. (2005).

The code for the BEAST analysis pipeline was written and executed on an IBM SP RS/6000 (*Seaborg*) at the National Energy Research Scientific Computing Center. The code was parallelized using MPI and ran on 640 processors. In order to obtain a stable PS estimate and to estimate our error bars to $\sim 20\%$ accuracy, we required 40 Monte Carlo runs. The operation count for our analysis pipeline scales approximately as $N_{\text{tod}} \log(N_{\text{tod}})$ with a large prefactor, where N_{tod} is the number of samples in the TOD.

In order to minimize the computational time, we modified the HEALPix routines SYNFAST (which makes a sky map from a power spectrum) and ANAFast (which calculates the power spectrum from a sky map) so that they only synthesize and analyze the portion of the sky where BEAST scans. Since the data set read in for the BEAST simulations is ~ 80 GB and the output maps for 40 MC runs are ~ 1.7 TB, we also implemented compression algorithms for storing the output maps on disk.

5. POWER SPECTRUM AND PARAMETER ESTIMATION

The CMB power spectrum extracted from the BEAST data is shown in Figure 5. The values of the power spectrum are shown in Table 1. The 1σ error bars shown in the figure should be interpreted with some caution. Forty Monte Carlo simulations allow

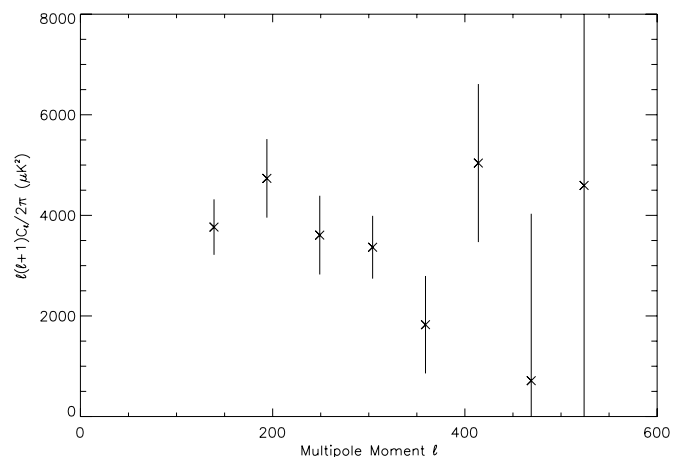


FIG. 5.—CMB anisotropy power spectrum for the BEAST experiment. Error bars are 1σ .

TABLE 1
BEAST POWER SPECTRUM ESTIMATES

Bin l_{\min}	Bin l_{\max}	Estimate in μK^2 of $l(l+1)C_l/2\pi$	1σ Error
139.....	193	3776	± 552
194.....	248	4744	± 781
249.....	303	3597	± 782
304.....	358	3374	± 625
359.....	413	1829	± 969
414.....	468	5040	± 1571
469.....	523	711	± 3319
524.....	678	4599	± 6136

NOTES.—The BEAST C_l estimates obtained using the MASTER method. The starting and ending values of each l bin are shown. The C_l -values in the table and those shown in Fig. 5 are averaged over these bins.

us to calculate these error bars to within 20%, which is sufficient for our purposes here, but more simulations would lead to more accurate error bars. In addition, we use the Monte Carlo simulations to calculate the transfer function (F_l), which is then used to produce the C_l estimates, and we use these same simulations to calculate the error bar on these estimates. Therefore, our estimate of the error bars on the power spectrum is not unbiased, and we underestimate the size of these error bars. In calculating our eight-binned C_l estimates, we effectively compute a binned transfer function T_b and a binned noise estimate N_b for each bin. We use 40 Monte Carlo simulations of noise to estimate N_b and 40 signal simulations to estimate T_b . Based on the number of degrees of freedom used to produce these eight-binned N_b and T_b , we estimate the bias in the error bar to be approximately 15%, of the same order as our Monte Carlo uncertainty in the errors. However, since this latter effect is a systematic bias, the comparison of the BEAST power spectrum estimates and the resulting parameter estimates to *WMAP* should be taken as “worst-case” consistency checks.

A χ^2 comparison of the BEAST data and the *WMAP* data was performed. For this comparison the *WMAP* data were assumed to have zero error. We find a χ^2 parameter of 15.02. With 9 degrees of freedom this means a larger value of χ^2 would occur approximately 10% of the time, so the BEAST power spectrum is marginally consistent with the *WMAP* result.

After the mean power spectrum was determined, its likelihood was sampled 40 times, producing 40 sample binned power spectra. The likelihood around the power spectrum is not, in general, Gaussian distributed, but through a change of variables—to the log-offset-normal variables of Bond, Jaffe, and Knox (BJK parameterization; Knox et al. 1998)—the distribution can be mapped into one that is much more nearly Gaussian. However, it was found that 40 samples of the power spectrum distribution was too few for a reliable determination of the BJK parameters, and thus it was decided that the power spectrum likelihood would be approximated as Gaussian-distributed. We then calculate the likelihood L of a theoretical power spectrum, D_i^{th} , as follows:

$$\chi^2 = \sum_{ij} (D_i^{\text{th}} - D_i^{\text{ob}}) M_{ij} (D_j^{\text{th}} - D_j^{\text{ob}}),$$

$$L = \exp(-\chi^2/2),$$

$$D_i^{\text{ob}} \equiv C_i^{\text{ob}} l(l+1)/2\pi,$$

where C_i^{ob} is the observed band-power of the i th bin, and M_{ij} is the covariance matrix.

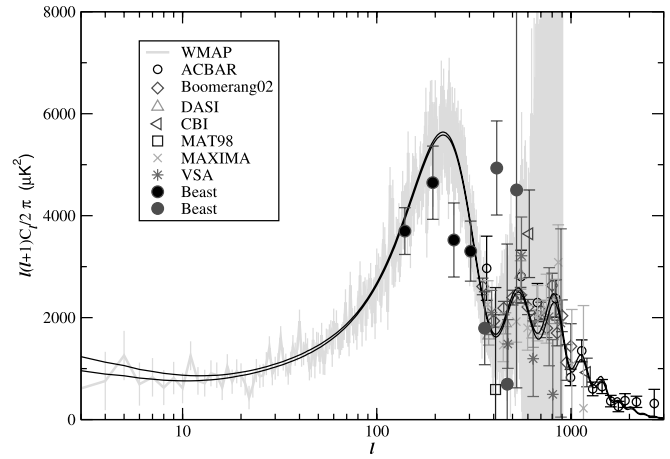


FIG. 6.—Data used for parameter estimation. For the *WMAP*+others analysis, only *WMAP* data were used over the range where it is cosmic variance limited. The four light gray BEAST circles were excluded along with all other data for $l < 350$. All points shown above $l = 350$ were used. All eight of the BEAST points plotted were used in the BEAST-only parameter estimation. The plot also allows comparison of the BEAST power spectrum to that of *WMAP*. [See the electronic edition of the Supplement for a color version of this figure.]

We determined the best-fit (maximally likely) points in parameter space for:

1. BEAST data + *WMAP* + MAXIMA, MAT, BOOMERANG, DASI, VSA, ACBAR, CBI + Hubble Key Project + big bang nucleosynthesis (BBN) relation between $\Omega_B h^2$ and He^4 mass fraction (Y_p) (Trota & Hansen 2004; Huey et al. 2004) over the parameter space: $\Omega_m, \Omega_\Lambda, h, n_s, \Omega_B h^2, Y_p, \tau, n_t, r$;
2. BEAST data alone.

For the BEAST + other recent cosmological data, we found the parameter values and errors via a Markov chain approach. Starting from a 30,000 point Markov chain previously run with the experiments *WMAP* + MAXIMA, MAT, BOOMERANG, DASI, VSA, ACBAR, CBI + Hubble Key Project + BBN $\Omega_B h^2$ - He^4 relation, the Markov chain was thinned by discarding 99 out of every 100 points. Each point was then weighted by the BEAST likelihood. From this weighted point distribution the parameter means and covariance matrix were determined. The parameter estimates were taken to be the means, and the parameter errors were taken as square roots of the diagonal elements of the covariance matrix. We show the BEAST power spectrum overlotted with a subset of points from the power spectra of several recent experiments in Figure 6. Only those points used

TABLE 2
COSMOLOGICAL PARAMETER ESTIMATES

Parameter	BEAST + Others
Ω_k	-0.014 ± 0.011
$\Omega_{\text{CDM}} h^2$	0.094 ± 0.012
$\Omega_b h^2$	0.024 ± 0.002
h	0.727 ± 0.048
n_s	1.002 ± 0.052
τ	0.154 ± 0.074
Y_p	0.249 ± 0.001

NOTES.—BEAST parameter estimates calculated using a joint analysis with other CMB data and BBN and Hubble Key Project constraints. $\Omega_k \equiv 1 - \Omega_{\text{tot}}$. The parameter errors were obtained from the variance of a Markov chain in parameter space. The results for BEAST alone produced only very weak constraints on the parameters.

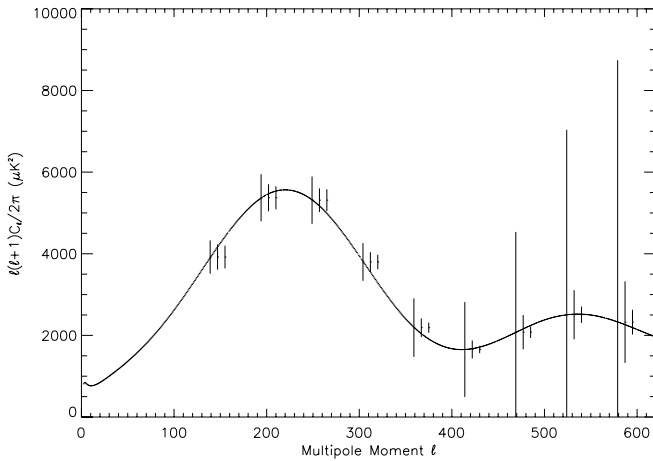


FIG. 7.—Effect on the power spectrum error bars of increasing the quantity of data to 4 and 16 times more data, effectively reducing the noise by factors of 2 and 4, respectively. The original error bars are plotted, followed by the half and quarter noise error bars. The original error bars are centered on the l bin, while the half and quarter noise are offset from the original position for illustrative purposes. In the analysis all of the error bars were calculated at the same l . The bin width in l is 55.

in our parameter estimation calculations are shown in the figure. In particular, for the joint analysis we include only *WMAP* for the l range in which *WMAP* is cosmic variance limited and discard the points from the other experiments. We include all of the BEAST data points for the BEAST-only analysis described below.

For BEAST data alone, cosmic parameter space was searched for the maximally likely point by first trying several candidate points, and then applying the Numerical Recipes Amoeba algorithm (Press et al. 1986) to minimize the trial χ^2 . The Amoeba algorithm has no inherent minimum scale (similar to adaptive mesh refinement, the resolution increases as necessary, with the precision limited only by the machine floating point arithmetic), and makes no assumptions about the shape of likelihood function.

Once the BEAST-alone best-fit cosmic parameters have been found, we determined the errors in these values. Ideally a method that, again, does not depend on the parameter likelihood function having a particular shape (i.e., Gaussian, for example), such as a Markov Chain algorithm, would be used. In this case however, a less computationally costly method can be employed. We determined the errors in the best-fit parameter values by fitting the likelihood function around that point to a multivariate Gaussian. The resulting estimate of the errors is crude, but sufficient to give an overall measure of the dispersion. To the extent to which the likelihoods are approximately Gaussian, in the narrowly constrained case (1) we expect these errors to be more accurate. The results of the joint parameter estimation for BEAST plus other experiments are shown in Table 2. We found the BEAST-alone parameters to be consistent with these values, although much less well constrained. For example, we found $\Omega_k \equiv 1 - \Omega_{\text{tot}} = -0.074 \pm 0.070$ for BEAST alone compared with -0.014 ± 0.012 for the joint estimate.

In order to examine possible future directions for the BEAST experiment, we analyzed the effect of increased quantities of data on the power spectrum error bars. A twofold and fourfold reduction in the simulated noise were considered, equating to 4 and 16 times more data, respectively, assuming no improvement in radiometer sensitivity. We found that over the first peak in the power spectrum there was not a significant improvement in the error bars with more data (see Fig. 7). This is expected, since in this region we are sample variance limited by the rel-

atively small patch of sky we observe. However, at larger l we do see a significant improvement in the power spectrum error bars, up to the point at which the experimental beam cuts off around an l of 600, when the error bars become large regardless of the amount of data.

6. CONCLUSIONS

We have presented the angular power spectrum of the cosmic microwave background as measured by the BEAST experiment. We have demonstrated that it is possible to extract cosmological signal from an easily accessible, ground-based CMB experiment that is dominated by correlated noise and that the resulting power spectrum and parameter estimation is consistent with previous results.

The MASTER method was successfully implemented and although this method is approximate, it proved to be flexible and robust and, in the final run, produced a power spectrum with less than 1000 CPU hours of computational time. The existence of the natural timescale for splitting the problem (55 minutes between instrument recalibrations) greatly simplified the parallelization of the BEAST analysis and provided a natural slicing when testing for systematics (e.g., even vs. odd hours). We believe the BEAST CMB data set to be one of the largest TODs analyzed to date, and this proved feasible within the MASTER framework. This suggests that the analysis of future, larger CMB data sets (e.g., *Planck*) should be computationally feasible.

We also analyzed how additional observing time would improve the power spectrum errors and found that significant improvements could be made between $250 \leq l \leq 600$ with additional time. We note that the atmospheric conditions at White Mountain allow for a better than 50% “good observing” fraction over the year.

This work was partially supported by the University of Illinois at Champaign-Urbana. This work has been partially supported by the National Computational Science Alliance under grant number AST020003N. This work was funded by NASA grants NAG5-4078, NAG5-9073, and NAG5-4185, and by NSF grants 9813920 and 0118297. In addition we were supported by the White Mountain Research Station, the California Space Institute (CalSpace), and the UCSB Office of Research. This research used resources of the National Energy Research Scientific Computing Center, which is supported by the Office of Science of the US Department of Energy under contract DE-AC03-76SF00098. The research described in this paper was carried out in part at the Jet Propulsion Laboratory, California Institute of Technology, under a contract with the National Aeronautics and Space Administration. J. M. is supported by FAPESP grants 01/13235-9 and 02/08471-1. T. V. and C. A. W. were partially supported by FAPESP grant 00/06770-2. T. V. was partially supported by CNPq grants 466184/00-0 and 302266/88-7-FA. C. A. W. was partially supported by CNPq grant 300409/97-4-FA and FAPESP grant 96/06501-4. We acknowledge the use of the Legacy Archive for Microwave Background Data Analysis (LAMBDA). Support for LAMBDA is provided by the NASA Office of Space Science. N. F. and A. P. were partially supported by CNPq grant number 470531/2001-0. B. D. W. acknowledges the 2003/4 NCSA Faculty Fellowship. Some of the results in this paper have been derived using HEALPix (Górski et al. 1998). We would like to thank Julian Borrill at NERSC for valuable discussions on the computational aspects of this project. We also thank members of the *Planck* community for stimulating discussions.

REFERENCES

- Bennett, C. L., et al. 2003, *ApJS*, 148, 1
- Childers, J., et al. 2005, *ApJS*, 158, 124
- Figueiredo, N., et al. 2005, *ApJS*, 158, 118
- Górski, K. M., Hivon, E., & Wandelt, B. D. 1998, in *Proc. MPA/ESO Conf. on Evolution of Large-Scale Structure: from Recombination to Garching*, ed. A. J. Banday, R. K. Sheth, & L. Da Costa (Garching: ESO), in press (astro-ph/9812350)
- Grainge, K., et al. 2003, *MNRAS*, 341, L23
- Halverson, N. W., et al. 2001, preprint (astro-ph/0104489)
- Hanany, S., et al. 2000, *ApJ*, 545, L5
- Hivon, E., Górski, K. M., Netterfield, C. B., Crill, B. P., Prunet, S., & Hansen, F. 2002, *ApJ*, 567, 2
- Huey, G., Cyburt, R. H., & Wandelt, B. D. 2004, *Phys. Rev. D*, 69, 103503
- Knox, L., Bond, J. R., Jaffe, A. H., Segal, M., & Charbonneau, D. 1998, *Phys. Rev. D*, 58, 83004
- Kolb, E. W., & Turner, M. S. 1990, *The Early Universe* (New York: Addison-Wesley)
- Kuo, C. L., et al. 2002, *BAAS*, 34, 1324
- Meinhold, P. M., et al. 2005, *ApJS*, 158, 101
- Mejia, J., et al. 2005, *ApJS*, 158, 109
- Miller, A. D., et al. 1999, *ApJ*, 524, L1
- Padin, S., et al. 2001, *ApJ*, 549, L1
- Peebles, P. J. E. 1993, *Principles of Physical Cosmology* (Princeton: Princeton Univ. Press)
- Press, W. H., Flannery, B. P., & Teukolsky, S. A. 1986, *Numerical Recipes: The Art of Scientific Computing* (Cambridge: Cambridge Univ. Press)
- Ruhl, J. E., et al. 2002, preprint (astro-ph/0212229)
- Trotta, R., & Hansen, S. H. 2004, *Phys. Rev. D*, 69, 023509
- Wandelt, B. D., Hivon, E. F., & Gorski, K. M. 2001, *Phys. Rev. D*, 64, 083003